Article

# Highly Selective Synthesis of the Ring-B Reduced Chlorins by Ferric Chloride-Mediated Oxidation of Bacteriochlorins: Effects of the Fused Imide vs Isocyclic Ring on Photophysical and Electrochemical Properties

Chao Liu, Mahabeer P. Dobhal, Manivannan Ethirajan, Joseph R. Missert, Ravindra K. Pandey, Sathyamangalam Balasubramanian, Dinesh K. Sukumaran, Min Zhang, Karl M. Kadish, Kei Ohkubo, and Shunichi Fukuzumi

*J. Am. Chem. Soc.*, **2008**, 130 (43), 14311-14323 • DOI: 10.1021/ja8050298 • Publication Date (Web): 02 October 2008



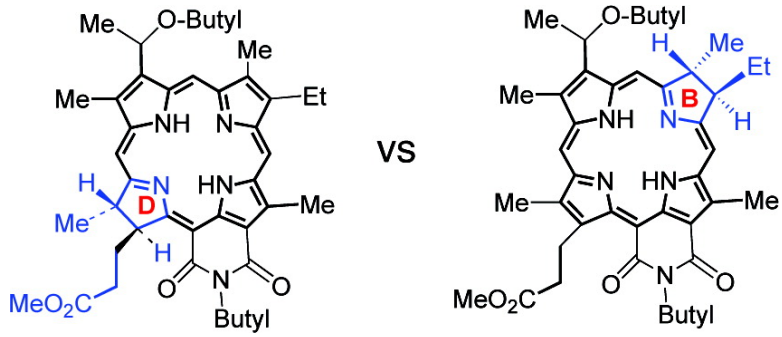


## More About This Article

Additional resources and features associated with this article are available within the HTML version:

- Supporting Information
- Access to high resolution figures
- Links to articles and content related to this article
- Copyright permission to reproduce figures and/or text from this article

View the Full Text HTML

J|A|C|S
ARTICLES

Published on Web 10/02/2008

# Highly Selective Synthesis of the Ring-B Reduced Chlorins by Ferric Chloride-Mediated Oxidation of Bacteriochlorins: Effects of the Fused Imide vs Isocyclic Ring on Photophysical and Electrochemical Properties

Chao Liu,[†] Mahabeer P. Dobhal,[†] Manivannan Ethirajan,[†] Joseph R. Missert,[†] Ravindra K. Pandey,*[,†] Sathyamangalam Balasubramanian,[‡] Dinesh K. Sukumaran,[‡] Min Zhang,[§] Karl M. Kadish,*[,§] Kei Ohkubo,[⊥] and Shunichi Fukuzumi*[,⊥]

*Chemistry Division, PDT Center, Cell Stress Biology, Roswell Park Cancer Institute, Buffalo, New York 14263, Pharmaceutical Sciences and Department of Chemistry, State University of New York, Buffalo, New York 14221, Department of Chemistry, University of Houston, Houston, Texas 77204-5003, and Department of Material and Life Science, Graduate School of Engineering, Osaka University, SORST, Japan Science and Technology Agency, Suita, Osaka 565-0871, Japan*

Received July 1, 2008; E-mail: ravindra.pandey@roswellpark.org; kkadish@uh.edu; fukuzumi@chem.eng.osaka-u.ac.jp

***Abstract:*** The oxidation of bacteriopyropheophorbide with ferric chloride hexahydrate or its anhydrous form produced the ring-D oxidized (ring-B reduced) chlorin in >95% yield. Replacing the five-member isocyclic ring in bacteriopyropheophorbide-*a* with a fused six-member *N*-butylimide ring system made no difference in regioselective oxidation, and the corresponding ring-B reduced chlorin was isolated in almost quantitative yield. When the oxidant was replaced by 2,3-dichloro-5,6-dicyano-*p*-benzoquinone, which is frequently used at the oxidizing stage of the porphyrin synthesis, the ring-B oxidized (ring-D reduced) chlorins were obtained. With both ring-B reduced and ring-D reduced chlorins in hand, their photophysical and electrochemical properties were examined and compared for the first time. The ring-B reduced chlorine **20**, with a fused six-member *N*-butylimide ring, exhibits the most red-shifted absorption band (at $\lambda_{max} = 746$ nm), the lowest fluorescence quantum yield (4.5%), and the largest quantum yield of singlet oxygen formation (67%) among the reduced ring-B and ring-D chlorins investigated in this study. Measurements of the one-electron oxidation and reduction potentials show that compound **20** is also the easiest to oxidize among the examined compounds and the third easiest to reduce. In addition, the 1.62 eV HOMO−LUMO gap of **20** is the smallest of the examined compounds, and this agrees with values calculated using the DFT method. Spectroelectrochemical measurements afforded UV−visible absorption spectra for both the radical cations and radical anions of the examined chlorins. The ring-B reduced compound **20**, with a fused six-member *N*-butylimide ring, is regarded as the most promising candidate in this study for photodynamic therapy because it has the longest wavelength absorption and the largest quantum yield of singlet oxygen formation among the compounds investigated.

## Introduction

Among tetrapyrroles, chlorophylls are the most abundant natural products on earth.[1] Chlorophyll biosynthesis is believed to take place in two phases.[2,3] The processes that take place in darkness in all plants are defined as "dark steps", whereas a light-dependent step and all subsequent steps are known as "late steps". At the later steps of biosynthesis, three types of chromophores can be distinguished: (i) porphyrins, (ii) chlorins (in which the pyrrole ring D is hydrogenated), and (iii) bacteriochlorins (in which the rings B and D are hydrogenated) (Figure 1). The enzyme protochlorophyllide oxidoreductase (POR) catalyzes the reduction of protochlorophyllide to chlorophyllide.[4] This reaction involves hydrogenation of one double bond in ring D by the hydrogen donor NADPH. However, it is not well understood why nature selected the ring-D reduced chlorin (chlorophyll-*a*) and the ring-B and ring-D reduced

[†] Roswell Park Cancer Institute.
[‡] State University of New York, Buffalo.
[§] University of Houston.
[⊥] Osaka University.

(1) Scheer, H. In *Chlorophylls and Bacteriochlorophylls: Biochemistry, Biophysics, Function and Applications*; Grimm, B., Porra, R. J., Rüdiger, W., Scheer, H., Eds.; Springer: Dordrecht, The Netherlands, 2006; Chapter 1, pp 1−26.
(2) Eckhardt, U.; Grimm, B. In *Handbook of Plant Science*; Robert, K., Ed.; John Wiley & Sons Ltd.: Chichester, UK, 2007; Vol. 2, pp 1224−1232.
(3) Bollivar, D. W. In *The Porphyrin Handbook*; Kadish, K. M., Smith, K. M., Guilard, R., Eds.; Elsevier: San Diego, 2003; Vol. 13, pp 49−69.
(4) Fujita, Y.; Bauer, C. E. In *The Porphyrin Handbook*; Kadish, K. M., Smith, K. M., Guilard, R., Eds.; Elsevier: San Diego, 2003; Vol. 13, pp 109−156.

  

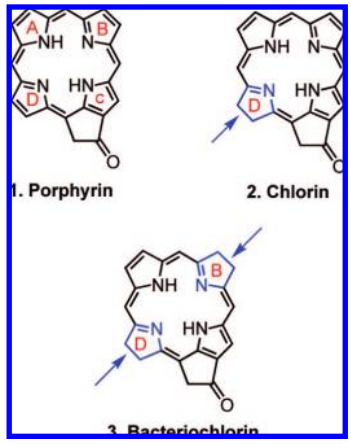


***Figure 1.*** Structures of porphyrin, chlorin, and bacteriochlorin systems (the reduced rings are indicated with blue arrows).

bacteriochlorins (bacteriochlorophyll-*a*) as chromophores in plant and bacterial photosynthetic reaction centers, respectively.[5]

One of the interesting characteristics of tetrapyrrole-based compounds is their ability to self-aggregate, which significantly impacts their optical properties.[6–8] This self-aggregation is influenced by the nature of the substituents at the peripheral position(s) of the molecule. Self-assemblies of $\pi$-conjugated moieties have attracted attention from the viewpoints of chemistry, biology, and material science.[6–11] Such assemblies are observed in various natural systems, especially bacteriochlorophylls stacked in photosynthetic organisms. X-ray crystallographic structural analysis of some bacteriochlorophyll-containing proteins has clearly shown $\pi-\pi$ stacking. On the other hand, self-aggregates of chlorophyllous pigments are found in light-harvesting antennas of green photosynthetic bacteria (chlorosomes) and have been studied in depth by various workers.[7,8] In collaboration with the Tamiaki group, we have shown that, similar to naturally occurring bacteriochlorophylls, the Zn(II) analogues of certain pyropheophorbide-*a* and purpurinimide (containing a six member N-substituted imide ring system) compounds self-aggregate to give large J-aggregates, which can be used as models of green photosynthetic bacterial chromosomes.[12]

Due to the long-wavelength absorptions of the chlorin and bacteriochlorin systems and their high singlet oxygen producing ability, the utility of these compounds in photodynamic therapy (PDT) has also been explored.[13,14] In our previous studies of structure−activity relationship (SAR) with a series of substituted chlorins (ring-D reduced porphyrins), we observed that, in addition to overall lipophilicity, the substituents at the various peripheral positions of the molecules make a significant difference in tumor uptake and PDT efficacy.[15,16] We have also shown that replacement of the five-member isocyclic ring in pyropheophorbide-*a* with a six-member fused *N*-substituted imide ring system (purpurinimide) produces a nearly 40−45 nm red-shift in the electronic absorption spectra. These ring-D reduced chlorins exhibit a long-wavelength absorption near 700 nm, which can be further red-shifted by introducing an electron-withdrawing group (−CHO or $-COCH_3$) at position 3 of the chromophores.[17]

Until now, most chlorin photosensitizers used in our laboratory have been derived from chlorophyll-*a*, which contains a reduced ring-D.[13–17] However, for quite some time, we have been interested in developing an efficient synthesis for the unsymmetrical chlorins related to pyropheophorbide-*a* and purpurinimides in which other rings (A, B, or C) are reduced instead of the pyrrole ring D. Our objective was (i) to study the impact of these structural isomers with similar overall lipophilicity in determining the PDT efficacy and (ii) to investigate their utility as synthetic models to understand more about the photosynthetic reaction centers. Why nature chose chlorophylls (ring-D reduced chlorins) in photosynthetic organisms as light-harvesting pigments in antenna complexes (LHC) and as electron carriers in reaction centers (RC) that carry out the light-driven electron transfer across the photosynthetic membrane is still an interesting puzzle.

We report herein a highly selective synthesis of ring-B reduced chlorins and examine the effects of the fused imide ring compared to the isocyclic ring on their photophysical and electrochemical properties. Our new approach for the preparation of such novel structures of chlorins should be of interest to both synthetic and physical chemists, as well as to those interested in the biological significance of these compounds.

## Results and Discussion

**Synthesis of Ring-B Reduced Chlorins.** For the synthesis of ring-B reduced chlorins, the bacteriopyropheophorbide-*a* **5**, which in turn was obtained from *Rhodobacter sphaeroides*, was selected as a substrate (Scheme 1). 2,3-Dichloro-5,6-dicyano-*p*-benzoquinone (DDQ), which has been frequently used at the oxidizing stage of the porphyrin synthesis either from a single pyrrole unit or from dipyrromethanes by following the MacDonald or tripyrrine or *a,c*-biladiene approach, was investigated for the oxidation of bacteriochlorin to chlorin. Unfortunately, the reaction of **5** with DDQ, which has also been widely used for the conversion of chlorins to porphyrins, especially for the conversion of chlorophyll analogues to various phylloerythrin derivatives (e.g., **9**, ring-D oxidized), mainly produced the ring-B

(5) Gomez-Maqueo, C. A.; Bryant, D. A. *Annu. Rev. Microbiol.* **2007**, *61*, 113–129.
(6) Smith, K. M.; Kehres, L. A.; Fajer, J. *J. Am. Chem. Soc.* **1983**, *105*, 1387–1389.
(7) Olson, J. M. *Photochem. Photobiol.* **1998**, *67*, 61–75.
(8) (a) Tamiaki, H. *Photochem. Photobiol. Sci.* **2005**, *4*, 675–680. (b) Tamiaki, H. *Coord. Chem. Rev.* **1996**, *148*, 183–197.
(9) Milgrom, L. R. *The Colours of Life*; Oxford University: Oxford, U.K., 1997; Chapter 7.
(10) (a) Hoeben, F. J. M.; Johkheijm, P.; Meijer, E. W.; Schenning, A. P. H. J. *Chem. Rev.* **2005**, *105*, 1491–1546. (b) Licha, K. *Top. Curr. Chem.* **2002**, *222*, 1–29.
(11) (a) Amao, Y.; Yamada, Y. *Biosens. Bioelectron.* **2007**, *22*, 1561–1565. (b) Stromberg, J. R.; Marton, A.; Kee, H. L.; Kirmaier, C.; Diers, J. R.; Muthiah, C.; Taniguchi, M.; Lindsey, J. S.; Bocian, D. F.; Meyer, G. J.; Holten, D. *J. Phys. Chem. C* **2007**, *111*, 15464–15478.
(12) Tamiaki, H.; Shimamura, Y.; Yoshimura, H.; Pandey, S. K.; Pandey, R. K. *Chem. Lett.* **2005**, *34*, 1344–1345.
(13) Pandey, R. K.; Zheng, G. In *The Porphyrin Handbook*; Kadish, K. M., Smith, K. M., Guilard, R., Eds.; Academic Press: Boston, 2000; Vol. 8, Chapter 43.
(14) Gryshuk, A.; Chen, Y.; Goswami, L. N.; Pandey, S.; Missert, J. R.; Tymish Ohulchanskyy, T.; Potter, W.; Prasad, P. N.; Allan Oseroff, A.; Ravindra, K.; Pandey, P. K *J. Med. Chem.* **2007**, *50*, 1754–1767.
(15) Pandey, R. K.; Sumlin, A. B.; Potter, W. R.; Bellnier, D. A.; Henderson, B. W.; Constantine, S.; Aoudia, M.; Rodgers, M. A. J.; Smith, K. M.; Dougherty, T. J. *Photochem. Photobiol.* **1996**, *52*, 194–205.
(16) Henderson, B. W.; Bellnier, D. A.; Greco, W. R.; Sharma, A.; Pandey, R. K.; Vaughan, L.; Weishaupt, K. R.; Dougherty, T. J. A. *Cancer Res.* **1997**, *47*, 4000–4007.
(17) Chen, Y.; Graham, A.; Potter, W.; Morgan, J.; Vaughan, L.; Bellnier, D. A.; Henderson, B. W.; Oseroff, A.; Dougherty, T. J.; Pandey, R. K. *J. Med. Chem.* **2002**, *45*, 255–258.

***Scheme 1.*** Synthesis of Bacteriopyropheophorbide-*a* **5** from Bacteriochlorophyll-*a*

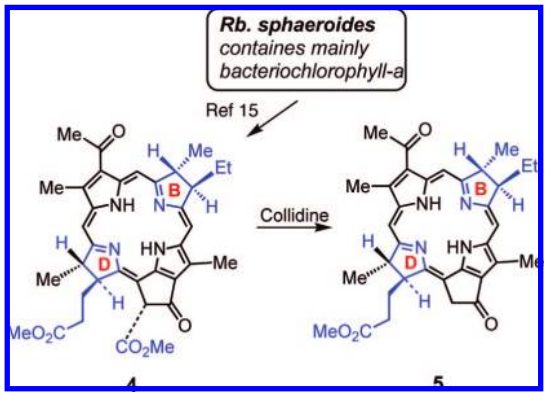


***Scheme 2.*** Conversion of Purpurinimide **8** and Pyroporphyrin **9** from Chlorophyll-*a*

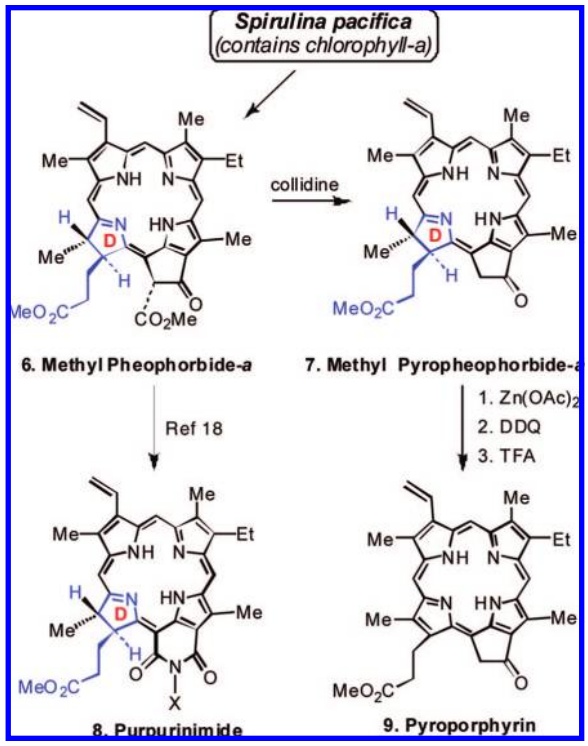


oxidized chlorin **10** (Scheme 3). Such observations were earlier reported by Tamiaki et al.[8] for the synthesis of methyl bacteriopheophorbide-*d* analogues from 3-acetyl-13[1]-oxo-bacteriochlorin.[19] We then explored the utility of other oxidizing agents, e.g., NIS and $H_5IO_6$, which unfortunately produced results similar to those obtained with DDQ oxidation. A further survey of the literature revealed the utility of several metal halides, especially ferric chloride hexahydrate, as convenient reagents for the oxidation of Hantzsch 1,4-dihydropyridines, as well as for the preparation of 4-alkoxy-2-arylquinolines, by an efficient oxidation of 2-aryl-1,2,3,4-tetrahydro-4-quinolines.[20,21]

***Scheme 3.*** Oxidation of Methyl Bacteriopyropheophorbide **5** with Various Oxidizing Agents

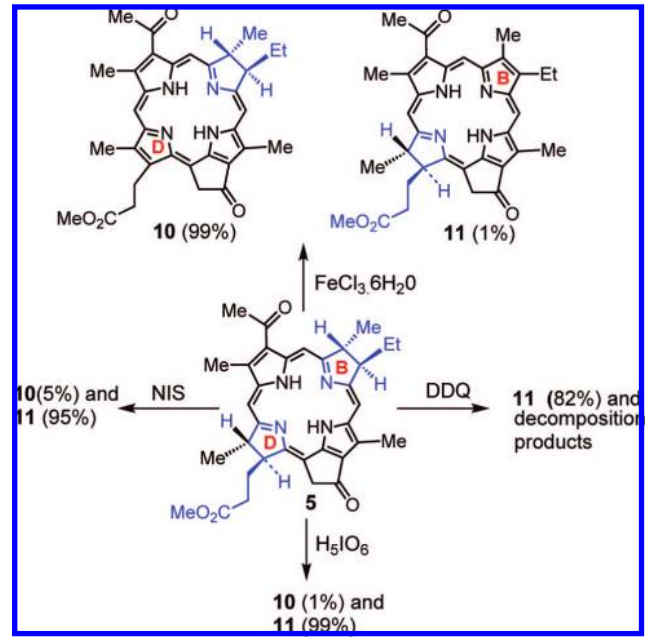


The utility of these reagents has recently been found to have value in porphyrin chemistry, especially for the regioselective oxidation of certain benzoporphyrins, as demonstrated by Lash and co-workers.[22] The Osuka group has also shown the application of $FeCl_3$ in the synthesis of quadruplynazulene-fused porphyrins.[23] Over 40 years ago, Smith and Calvin investigated the chemical and photochemical oxidation of bacteriochlorophyll, and various oxidized products, including chlorophyll-*a*, were isolated.[24] That group also reported the use of ferric chloride for oxidation of bacteriochlorophylls, which gave mainly the decomposition products. In contrast, in our hands the oxidation of bacteriopyropheophorbide with ferric chloride hexahydrate or its anhydrous form mainly produced the ring-D oxidized (ring-B reduced) chlorin **10** in 99% yield. Replacing the five-member isocyclic ring present in bacteriopyropheophorbide-*a* **5** with a fused six-member *N*-butylimide ring system **12** did not make any difference in regioselective oxidation, and the corresponding ring-B reduced chlorin **13** was isolated in almost quantitative yield (Scheme 4).

On the basis of SAR and quantitative structure−activity relationship (QSAR) studies, we have been able to identify the most effective candidates as **17** and **18** from the pyropheophorbide and bacteriopurpurinimide series with limited skin phototoxicity, a main drawback associated with most of the porphyrin-based compounds including Photofrin (Axcan Pharma Inc.,), a currently FDA-approved PDT agent.[25] These new photosensitizers are currently at various stages of human clinical/preclinical trials.

(18) (a) Zheng, G.; Potter, W. R.; Camacho, S. H.; Missert, J. R.; Wang, G.; Bellnier, D. A.; Henderson, B. W.; Rodgers, M. A. J.; Dougherty, T. J.; Pandey, R. K. *J. Med. Chem.* **2001**, *44*, 1540–1559. (b) Zheng, G.; Potter, W. R.; Sumlin, A.; Dougherty, T. J.; Pandey, R. K. *Bioorg. Med. Chem. Lett.* **2000**, *10*, 123–127.
(19) Tamiaki, H.; Kouraba, M.; Takeda, K.; Kondo, S.; Tanikaga, R. *Tetrahedron: Asymmetry* **1998**, *9*, 2101–2111.
(20) Diaz Diaz, D.; Miranda, P. O.; Padron, J. I.; Martin, V. S. *Curr. Org. Chem.* **2006**, *10*, 457–476.
(21) Kumar, K. H.; Muralidharan, D.; Perumal, P. T. *Tetrahedron Lett.* **2004**, *45*, 7903–7906.
(22) (a) Hayes, M. J.; Spence, J. D.; Lash, T. D. *Chem. Commun.* **1998**, 2409–2410. (b) Lash, T. D.; Muckey, M. A.; Hayes, M. J.; Liu, D.; Spence, J. D.; Ferrence, G. M. *J. Org. Chem.* **2003**, *68*, 8558–8570.
(23) Kurotobi, K.; Kim, K. S.; Noh, S. B.; Kim, D.; Osuka, A. *Angew. Chem., Int. Ed.* **2006**, *45*, 3944–3947.
(24) Lindsay Smith, J. R.; Calvin, M. *J. Am. Chem. Soc.* **1966**, *88*, 4500–4506.

***Scheme 4.*** Regioselective Oxidation of 3-Acetyl-bacteriopurpurinimide to the Corresponding Ring-B Reduced *N*-Butyl-purpurinimide

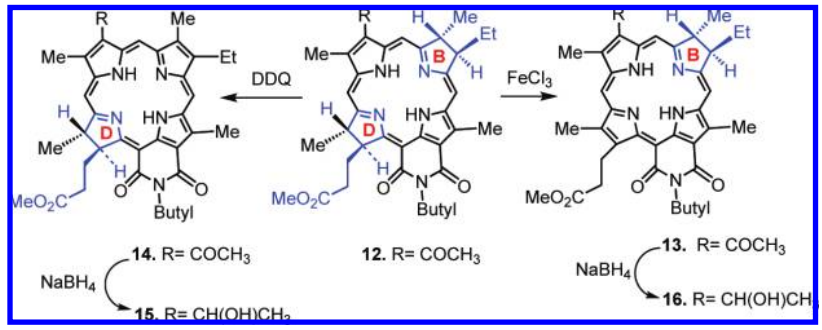


***Scheme 5.*** Regioselective Synthesis of Ring-B Reduced Chlorins **19** and **20**, Respective Isomers of Highly Effective Ring-D Reduced Chlorins **17** and **18**

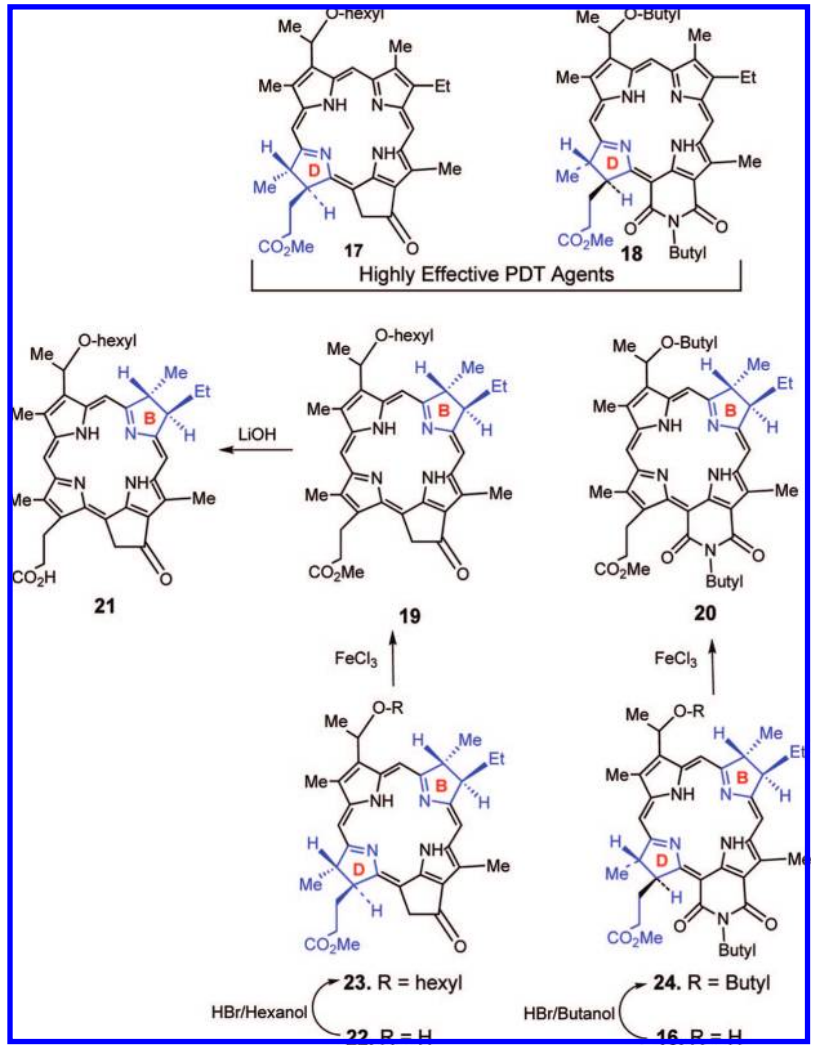


After discovering the use of $FeCl_3$ in regioselective oxidation of bacteriochlorins, we were interested in synthesizing the ring-B reduced chlorins **19** and **20** and then comparing their efficacy with that of the corresponding ring-D reduced chlorins **17** and **18**, respectively. The synthesis of the desired isomers is shown in Scheme 5. In brief, 3-acetyl-bacteriopyropheophorbide-*a* and 3-acetyl-*N*-butyl-bacteriopurpurinimide were prepared by following the methodology established in our laboratory. Reduction of the acetyl group at position 3 and subsequent treatment with HBr gas and the appropriate alcohols (**22**, **16**) afforded the bacteriochlorins **23** and **24**, which on treatment with ferric chloride gave the desired ring-B reduced chlorins **19** and **20**, respectively.

The course of the reaction could be followed by monitoring changes in the absorption spectrum, and some interesting differences between the electronic absorption spectra of the ring-B and ring-D reduced isomers were observed. As can be seen from Figure 2a, the two chlorins showed similar characteristics, and the long-wavelength absorption bands were observed at $\lambda_{max} = 683$ and 690 nm for **11** and **10**, respectively. In both chlorins, on replacing the electron-withdrawing acetyl groups at position 3 with 3-(1-butyloxyethyl) analogues **18** and

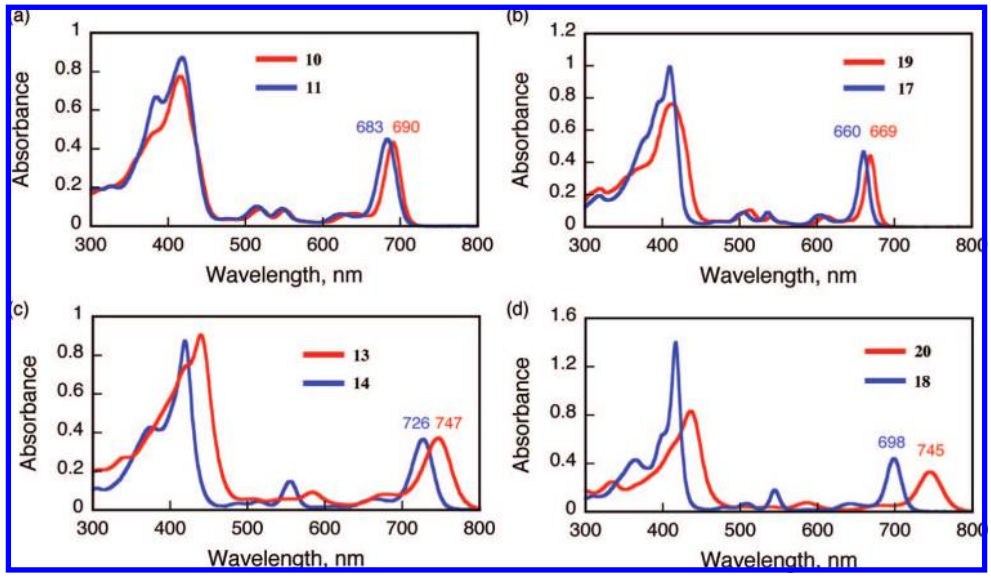


***Figure 2.*** Electronic absorption spectra of chlorins with ring-B and ring-D reduced isomers: (a) **10** and **11**, (b) **17** and **19**, (c) **13** and **14**, and (d) **18** and **20**. Red spectra denote the ring-B reduced chlorins (**10**, **13**, **19**, and **20**). Blue spectra denote the ring-D reduced chlorins (**11**, **14**, **17**, and **18**).

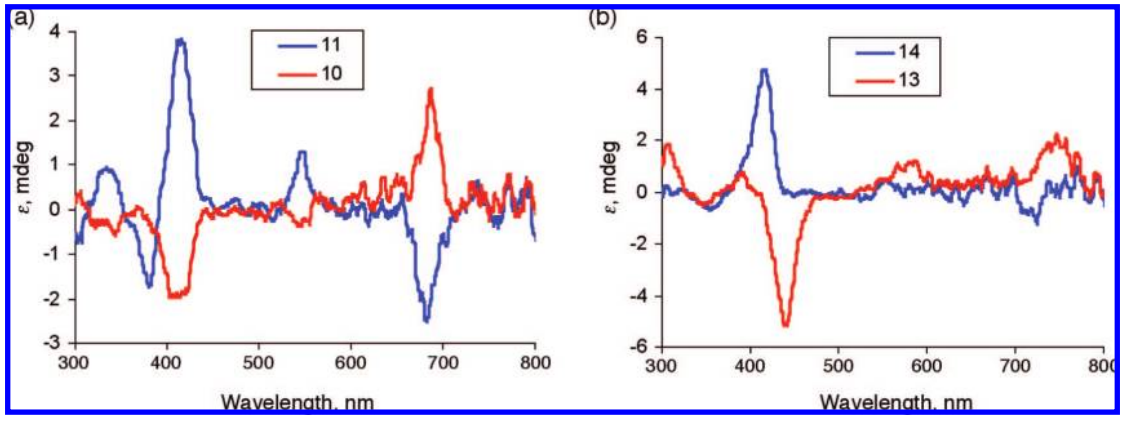


***Figure 3.*** CD spectra of chlorins (a) **10** and **11** (pyro series) and (b) **13** and **14** (purpurinimide series) in dichloromethane (concentration 10 $\mu$M).

**20**, a significant blue-shift was seen in the absorption spectra: the long-wavelength absorptions of these chromophores were observed at 698 and 746 nm, respectively (Figure 2d). As expected, replacement of the acetyl substituent with a hexyloxyethyl group at position 3 in both of the chlorins **17** and **19** resulted in a blue-shift in the spectra: the long-wavelength absorptions were observed at 660 and 669 nm, respectively, as shown in Figure 2b. Replacing the isocyclic ring present in chlorins **10** and **11** with six-member imide ring systems **13** (pyrrole ring-B reduced) and **14** (pyrrole ring-D reduced) led to a strong red-shift: the long-wavelength peaks were observed at 747 and 726 nm, respectively. Thus, compared to the ring-D reduced chlorin **14**, the corresponding ring-B analogue **13** showed a red-shift of 21 nm (Figure 2c). As expected, replacing the electron-withdrawing acetyl group at position 3 with a 1-butyloxyethyl substituent in ring-D reduced chlorin **18** led to a 47 nm blue-shift, similar to that observed in chlorins **17** and **19**. However, to our surprise, no such shift was observed between the electronic absorption spectra of the acetyl chlorin **13** and the corresponding 1-butyloxyethyl analogue **20** (Figure 2c,d).

**Circular Dichroism Results.** Compounds **10** and **11** (Figure 3) exhibit circular dichroism (CD) spectra with bands at 690, 550, 420, and 390 nm and one at 340 nm. The observation of a band around 700 nm is consistent with the presence of a fused purpurinimide ring. However, the sign of these bands is opposite for compounds **10** and **11**, suggesting optical activity differences between these two molecules. For example, in compound **10**, the band at 690 nm is observed as a positive band, possibly due to the reduction of ring D, but it reverses its sign to become a negative band in ring-B reduced chlorin. The data clearly suggest that these substitutions cause conformational changes in the chlorin. Further analysis of the spectra suggests the existence of exciton splitting, indicating self-association of the molecules. Comparing the spectral properties of compounds **10** and **11** with those of **13** and **14** reveals that both sets of compounds show bands at similar locations, indicating similar conformation. Similar to what is observed for compounds **10** and **11**, the band at 690 nm in compounds **13** and **14** reverses in sign, depending upon the stereochemical and conformational changes involving reduction at rings B and D. However, for compounds **13** and **14**, the bands observed at 550 and 690 nm are not as intense as in compounds **10** and **11**. This may be due to alterations in the $\pi-\pi$ interaction between neighboring molecules owing to an inductive effect of the butyl moiety in compounds **13** and **14**.

**NMR Studies.** Compounds **10**, **11**, **13**, and **14** were fully characterized by 1D ($^1$H) and 2D (COSY, NOESY, ROESY)

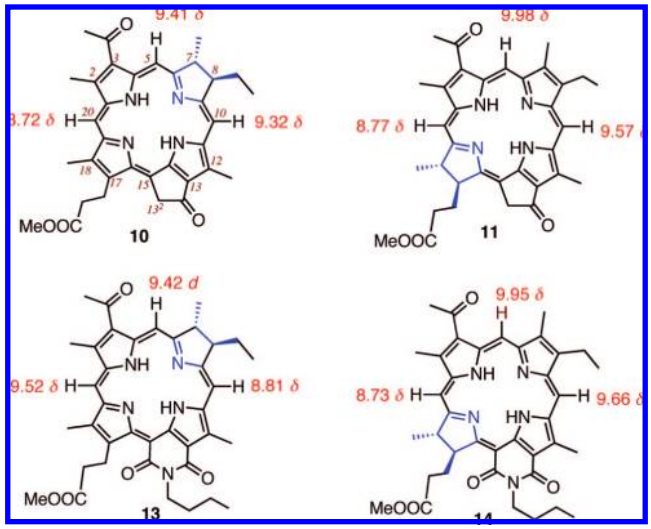


***Figure 4.*** $^1$H NMR values of *meso*-protons for **10**, **11** and **13**,**14**.

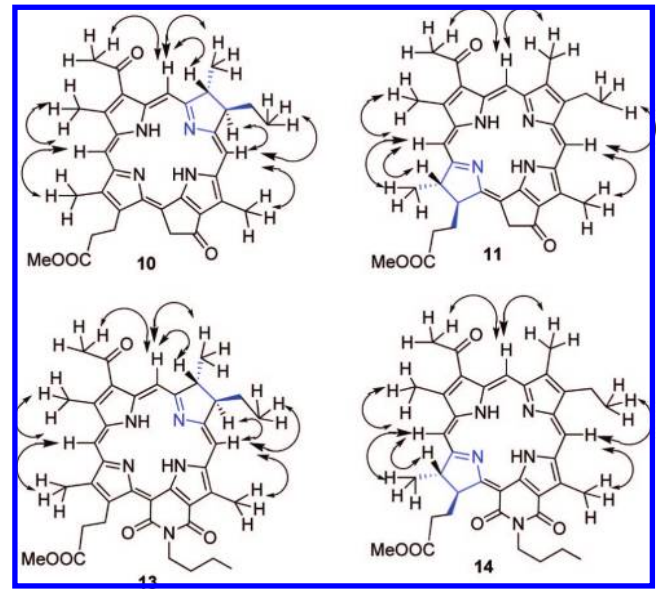


***Figure 5.*** NOE correlations of the *meso*-protons for **10**, **11** and **13**, **14**.

NMR techniques and also by HRMS-ESI analyses. Among these chlorins, methyl 3-acetyl-3-devinyl-pyropheophorbide-*a* **11** is a known chlorin, and our NMR assignments are similar to those reported in the literature.[26] It is well established in the literature that tetrapyrrolic systems with reduced pyrrole unit exhibit a significant difference in the electronic properties of the molecule as compared to the unreduced form of the compound, and the *meso*-protons next to the reduced ring show downfield shifts. As expected, the 20-H *meso*-proton (next to reduced ring D) in compound **11** appears at $\delta$ 8.77. The 5- and 10-*meso*-protons are observed at $\delta$ 9.98 and 9.57, respectively. However, to our surprise, no such correlation was observed in the ring-D reduced chlorin **10**. Interestingly, the *meso*-protons next to the reduced pyrrole ring D appear at $\delta$ 8.72 and thus show a significant upfield shift compared to the *meso*-proton at position 20 (Figure 4).

To confirm the structural assignment for **10**, the resonances for the ethyl group at position 8 were chosen as a starting point for the interpretation of the NOESY results. A triplet at $\delta$ 1.16 for the $CH_2CH_3$ protons showed NOE correlation with the adjacent *meso*-proton at $\delta$ 9.32; the $-CH_2$ protons of the ethyl group also showed a strong interaction with the adjacent *meso*-proton. Hence, the singlet at $\delta$ 9.32 is assigned to 10-H. The 10-C*H* proton is also found to interact with the 12-$CH_3$ protons which appear at $\delta$ 3.70. Furthermore, the close correlation of the 7-$CH_3$ protons and the acetyl protons with 5-H ($\delta$ 9.41) confirms the proposed structural assignment for **10**. By following a similar approach, the resonances at $\delta$ 8.72 are assigned to the *meso*-proton at position 20. The NOE interactions between the peaks at $\delta$ 3.85 and 2.92 were of crucial importance in assigning the structure. For example, strong NOE cross peaks between 17-$CH_2$- and 13$^1$-$CH_2$ (these appear as a singlet instead of the ABX pattern observed in the ring-D reduced chlorin **11**) further confirm the structure of ring-B reduced chlorin **10**.

We extended this approach in examining structures of the ring-D and ring-B reduced purpurinimides **13** and **14**. Interestingly, and in contrast to chlorin **10**, the *meso*-protons next to the reduced ring in both chlorins **13** and **14** show a downfield shift in their resonances. For the ring-B reduced chlorin **13**, the NOE cross peaks between the 7$^1$-$CH_3$ and $\delta$ 9.42 assigned to the 5-H *meso*-proton. This was further confirmed by its NOE interaction with the acetyl protons at position 3. The NOE correlation of the singlet appearing at $\delta$ 9.52 with the 2-$CH_3$ as well as the 18-$CH_3$ protons assigned the resonances to the 20-H *meso*-proton. The singlet observed at $\delta$ 8.81 showed interactions with 8-H and 8$^1$-C$H_2$ as well as the 12-C$H_3$ protons and is assigned to the *meso*-proton at position 10, thus confirming unequivocally the structure of the ring-B reduced purpurinimide **13**. The other NOE correlations, useful in the complete assignment of the compounds **10**, **11**, **13**, and **14**, are shown in Figure 5.

**Fluorescence Spectra and Quantum Yields.** Fluorescence spectra of the chlorin compounds are shown in Figure 6 along with the fluorescence quantum yields ($\Phi$). The fluorescence of the ring-B reduced purpurinimide (**20**) in Figure 6b is significantly red-shifted as compared with that of the ring-D reduced purpurinimide (**18**) in Figure 6a. This is in agreement with the absorption spectra in Figure 1. The fluorescence quantum yield of **20** (0.045) is significantly smaller than that of **18** (0.070). In contrast, the fluorescence quantum yield of the ring-B reduced chlorin with the five-member isocyclic ring **19** is only slightly red-shifted as compared with that of the corresponding ring-D reduced chlorin **17**, in accordance with their absorption spectra. The fluorescence quantum yield of **19** (0.23) is larger than that of **17** (0.19).

Fluorescence decay-time profiles of the chlorins are shown in Figure 7. In each case, the decay is well fitted to a single-exponential curve, indicating that each chlorin is pure and no aggregation occurs under the present experimental conditions. The fluorescence lifetimes of the ring-B reduced chlorins **19** and **20** are somewhat shorter than those of the corresponding ring-D reduced chlorins **17** and **18**. In accordance with the larger fluorescence quantum yields of the chlorins with a five-member isocyclic ring (**17** and **19**) as compared with those of the chlorins

(25) Chen, Y.; Potter, W. R.; Missert, J. R.; Morgan, J.; Pandey, R. K. *Bioconjugate Chem.* **2007**, *18*, 1460–1473.
(26) Tamiaki, H.; Shiki, Y.; Miyatake, T. *Bioorg. Med. Chem.* **1998**, *6*, 2171–2178.

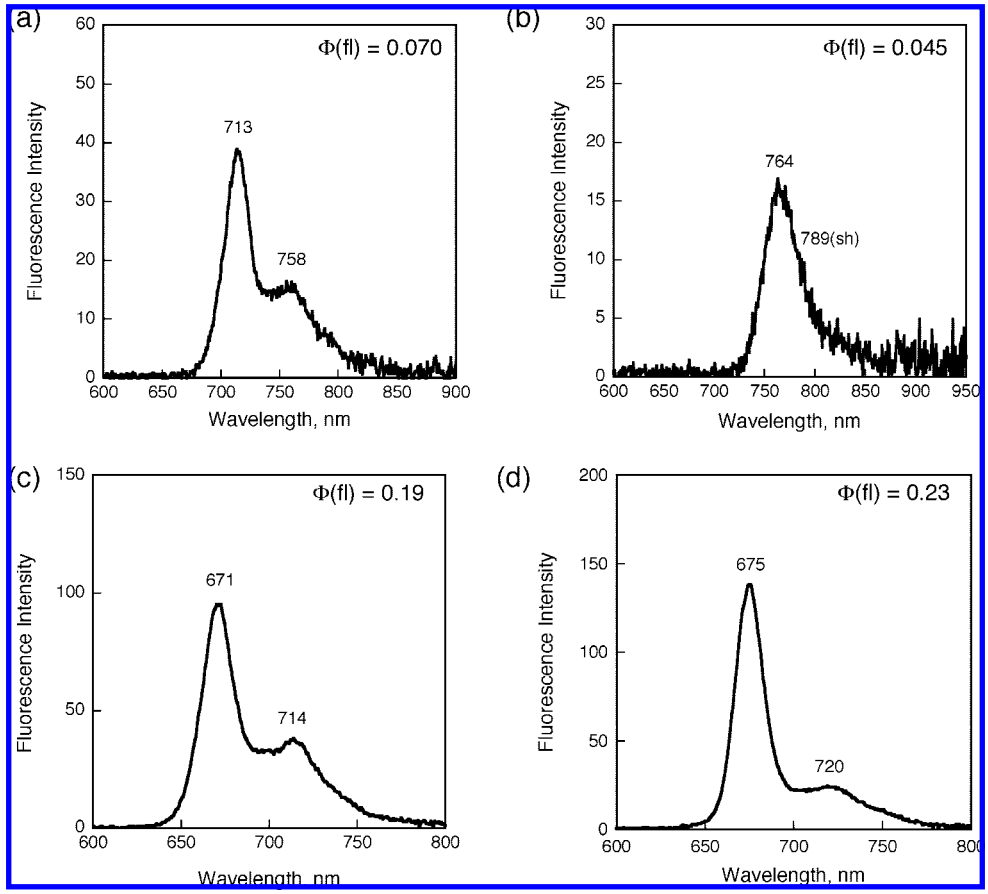


***Figure 6.*** Fluorescence spectra of chlorins with ring-B and ring-D reduced isomers: (a) purpurinimide **18** ($\lambda_{ex}$ = 417 nm), (b) isomer of purpurinimide **20** ($\lambda_{ex}$ = 437 nm), (c) HPPH methyl ester **17** ($\lambda_{ex}$ = 410 nm), and (d) isomer of HPPH methyl ester **19** ($\lambda_{ex}$ = 413 nm), in PhCN.

**18** and **20**, the fluorescence lifetimes of **17** and **19** are significantly longer than those of **18** and **20**.[27]

**Formation of Singlet Oxygen.** Irradiation of an oxygen-saturated benzene solution of each chlorin results in formation of singlet oxygen, which was detected by the $^1O_2$ phosphorescence at 1270 nm.[28,29] The quantum yields of $^1O_2$ generation for each compound were determined from the phosphorescence intensity, referred to the intensity of $C_{60}$ ($\Phi$ = 0.96).[30,31] The measured quantum yields of singlet oxygen [$\Phi(^1O_2)$] are shown in Figure 8. The largest $\Phi$ value (67%) is obtained for the ring-B reduced purpurinimide. The $\Phi$ values of the ring-B reduced chlorins **19** and **20** are slightly larger than those of the corresponding ring-D reduced chlorins **17** and **18**.

**Highest Occupied and Lowest Unoccupied Molecular Orbitals of Chlorins.** The HOMO and LUMO of the chlorins were calculated using density functional theory (DFT) with the B3LYP density functional[32] and the 3-21G* basis set. All calculations were performed using GAUSSIAN-03.[33] The results are shown in Figure 9. No electron is delocalized on the $\beta$-position of the reduced B or D ring in the HOMO, whereas electron density is delocalized on the oxidized the $\beta$-position of the reduced B or D rings. In the LUMO, no coefficient is seen on the $\beta$-position of reduced D ring or the oxidized B ring of **18**, whereas the delocalization is recognized on the $\beta$-position of the oxidized D ring of **20**. This results in a smaller HOMO−LUMO gap of the ring-B reduced purpurinimide **20** (2.17 eV) as compared with the gap of the ring-D reduced purpurinimide **18** (2.37 eV). In the case of chlorins with the five-member isocyclic ring, the HOMO−LUMO gap is the same for the ring-B reduced chlorin (**19**) and the ring-D reduced chlorin (**17**), and the value (2.52 eV) is larger than that of the purpurinimide isomers (see Figure S5 in the Supporting Information).

**Redox Processes.** The electrochemistry of each free-base chlorin was investigated in dichloromethane ($CH_2Cl_2$) containing 0.1 M TBAP as supporting electrolyte. Each compound undergoes two reversible reductions and two oxidations, only the first of which is reversible. Cyclic voltammograms of **18**

(27) The smaller fluorescece quantum yield with the longer fluorescence lifetime than those of **19** may result from faster nonradiative relaxation of **17** under the present experimental conditions.

(28) (a) Araki, Y.; Dobrowolski, D. C.; Goyne, T. E.; Hanson, D. C.; Jiang, Z. Q.; Lee, K. J.; Foote, C. S. *J. Am. Chem. Soc.* **1984**, *106*, 4570–4575. (b) Fukuzumi, S.; Fujita, S.; Suenobu, T.; Yamada, H.; Imahori, H.; Araki, Y.; Ito, O. *J. Phys. Chem. A* **2002**, *106*, 1241–1247.
(29) Fukuzumi, S.; Ohkubo, K.; Zheng, X.; Chen, Y.; Pandey, R. K.; Zhan, R.; Kadish, K. M. *J. Phys. Chem. B* **2008**, *112*, 2738–2746.
(30) Abogast, J. W.; Darmanyan, A. P.; Chrostopher, P. D.; Foote, C. S.; Rubin, Y.; Diederich, F. N.; Alvarez, M. M.; Anz, S. J.; Whetten, R. L. *J. Phys. Chem.* **1991**, *95*, 11–12.
(31) Chen, Y.; Ohkubo, K.; Zhang, M.; E, W.; Liu, W.; Pandey, S. K.; Ciesielski, M.; Baumann, H.; Fukuzumi, S.; Kadish, K. M.; Fenstermaker, R.; Oseroff, A.; Pandey, R. K *Photochem. Photobiol. Sci.* **2007**, *6*, 1257–1267.
(32) Becke, A. D. *J. Chem. Phys.* **1993**, *98*, 5648–5652.
(33) Frisch, M. J.; et al. *Gaussian 03*, Revision C.02; Gaussian, Inc.: Wallingford, CT, 2004.

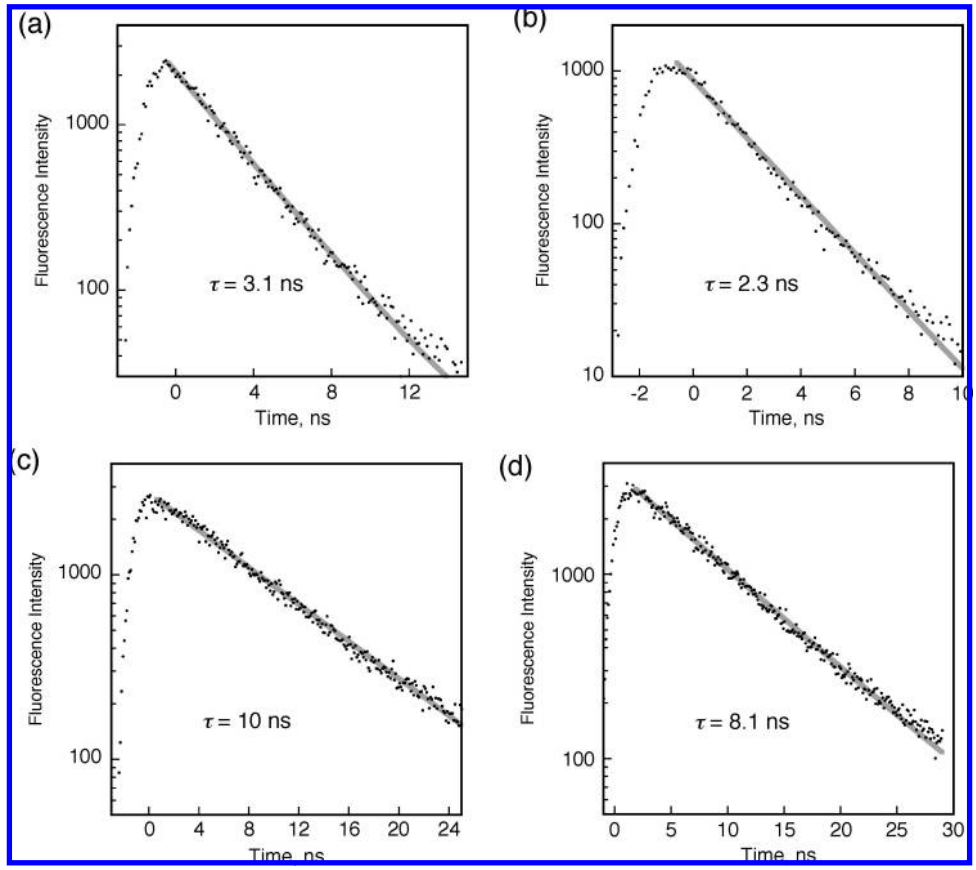


***Figure 7.*** Fluorescence lifetimes of chlorins with ring-B and ring-D reduced isomers: (a) purpurinimide (**18**), (b) purpurinimide isomer (**20**), (c) HPPH methyl ester (**17**), and (d) isomer of HPPH methyl ester-B (**19**).

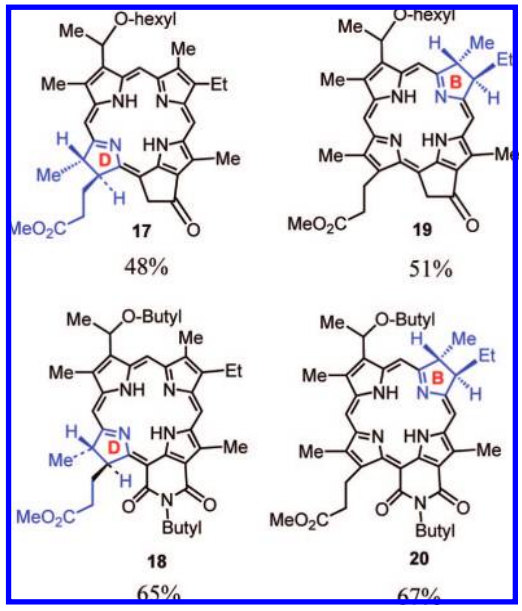


***Figure 8.*** Singlet oxygen quantum yields of chlorins with ring-B and ring-D reduced isomers in $C_6D_6$: (a) purpurinimide (**18**), (b) isomer of purpurinimide (**20**), (c) HPPH methyl ester (**17**), and (d) isomer of HPPH methyl ester (**19**).

and **20** are shown in Figure 10, and the half-wave potentials for each redox process are summarized in Table 1.

The four compounds with a six-atom fused exocyclic ring (**13**, **14**, **18**, and **20**) are easier to reduce than those with a five-atom fused exocyclic ring (**10**, **11**, **17**, and **19**), but there are no significant differences in $E_{1/2}$ values for the first oxidation. Thus, the potential separation in $E_{1/2}$ values between the first reversible reduction and first reversible oxidation (HOMO−LUMO gap) of the compounds with a five-atom exocyclic ring is larger than that for the compounds with a six-atom ring. This is seen in Table 1 and agrees with the calculated HOMO−LUMO gaps (vide supra).

Compounds **18** and **20** have a six-atom fused exocyclic ring and a substituted butyloxyethyl substituent, while compounds **14** and **13** possess an acetyl substituent at the same position of the chlorin macrocycle. Compounds **17** and **19** have a five-atom exocyclic ring and hexyloxyethyl substituents, while **11** and **10** have a five-atom exocyclic ring and one acetyl substituent. As seen in Table 1, the four compounds with an acetyl group are all easier to reduce and harder to oxidize than the four compounds with a butyloxyethyl or hexyloxyethyl substituent and the same exocyclic ring; this is expected because the acetyl substituent is an electron-withdrawing group.

The main difference between the ring-B and ring-D reduced isomers is in the different $\pi$-conjugated ring systems. In general, the compounds with a reduced ring B are easier to reduce and easier to oxidize than those with a reduced ring D which have the same fused exocyclic ring and the same substituents. This is not the case for compounds **17** and **19**, which have almost the same redox potentials for each electron-transfer process, thus indicating that the reduced D and B rings have no effect on the electrochemistry of these two compounds.

**Spectroelectrochemistry.** Spectroelectrochemical monitoring of the redox processes was carried out for the first oxidation and first reduction of the eight compounds in $CH_2Cl_2$

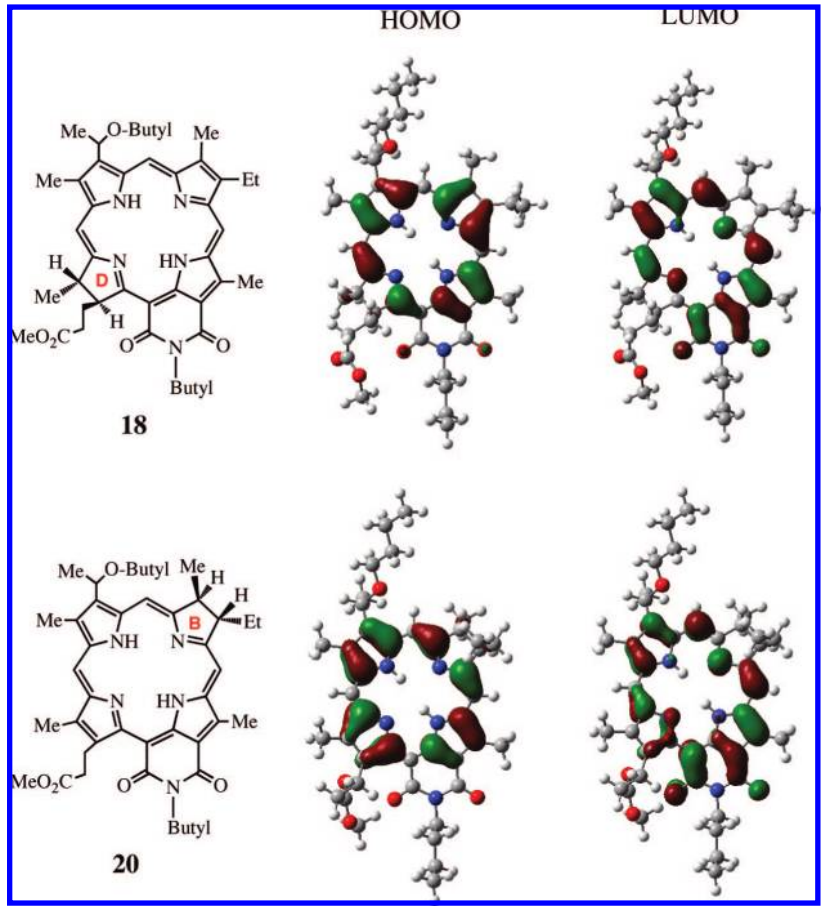


***Figure 9.*** HOMOs and LUMOs of purpurinimide **18** (ring-D reduced) and its isomer **20** (ring-B reduced).

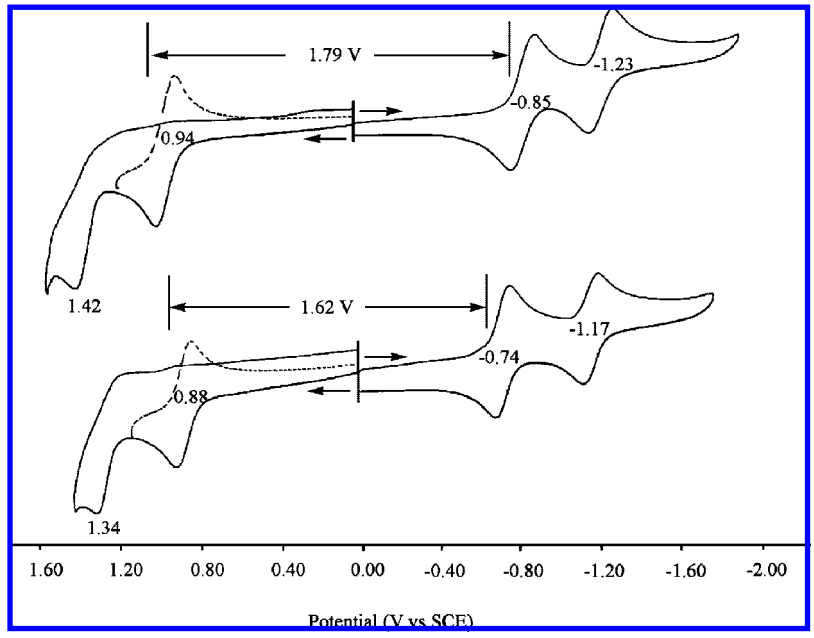


***Figure 10.*** Cyclic voltammograms of compounds **18** (top) and **20** (bottom) in $CH_2Cl_2$ containing 0.1 M TBAP.

containing 0.2 M TBAP as supporting electrolyte. The UV−visible spectroscopic data for the neutral and singly reduced or singly oxidized chlorins are summarized in Table 2. Each investigated compound has six absorption bands between 300 and 1000 nm. One interesting feature is the large difference (21−47 nm) in the long-wavelength absorption band between the chlorins with a six-atom fused exocyclic ring and those with reduced B or D ring (**18** and **20**, **14** and **13**). Much smaller differences in UV−visible spectra are seen for the neutral compounds with a five-atom fused exocyclic

***Table 1.*** Half-Wave Potentials (V vs SCE) of Investigated Free-Base Chlorins in $CH_2Cl_2$, 0.1 M TBAP

| compd | exocyclic ring | substituent | reduced ring | oxidation 2nd | oxidation 1st | reduction 1st | reduction 2nd | HOMO−LUMO gap |
|---|---|---|---|---|---|---|---|---|
| **18** | six atom | butyloxyethyl | D | 1.42[a] | 0.94 | −0.85 | −1.23 | 1.79 |
| **20** | six atom | butyloxyethyl | B | 1.34[a] | 0.88 | −0.74 | −1.17 | 1.62 |
| **14** | six atom | acetyl | D | 1.53[a] | 1.04 | −0.67 | −1.02 | 1.71 |
| **13** | six atom | acetyl | B | 1.45[a] | 1.02 | −0.63 | −0.98 | 1.65 |
| **17** | five atom | hexyloxyethyl | D | 1.34[a] | 0.88 | −1.10 | −1.37 | 1.98 |
| **19** | five atom | hexyloxyethyl | B | 1.32[a] | 0.87 | −1.11 | −1.37 | 1.98 |
| **11** | five atom | acetyl | D | 1.36[a] | 0.96 | −0.94 | −1.10 | 1.90 |
| **10** | five atom | acetyl | B | 1.38[a] | 0.95 | −0.92 | −1.09 | 1.87 |

[a] Peak potential at scan rate = 0.10 V/s.

***Table 2.*** UV−Visible Data ($\lambda$, nm) for Neutral, First Reduced and First Oxidized Investigated Free-base Chlorins in $CH_2Cl_2$ Containing 0.2 M TBAP

| compd | neutral | 1st reduction | 1st oxidation |
|---|---|---|---|
| **18** | 362, 417, 509, 546, 641, 698 | 328, 601, 732, 799 | 411, 666, 780 |
| **20** | 334, 437, 538, 587, 683, 745 | 307, 419, 450, 876 | 441, 708, 830 |
| **14** | 377, 419, 514, 555, 656, 726 | 644, 784, 826 | 421, 684 |
| **13** | 416, 438, 539, 584, 676, 747 | 636, 788, 876 | 443, 698 |
| **17** | 318, 410, 505, 538, 604, 660 | 629, 779 | 413, 651, 792 |
| **19** | 319, 413, 513, 541, 612, 669 | 339, 620, 798 | 422, 655, 780 |
| **11** | 386, 417, 515, 547, 624, 683 | 483, 626, 817 | 428, 644 |
| **10** | 382, 415, 519, 551, 639, 690 | 343, 646, 850 | 427, 666 |

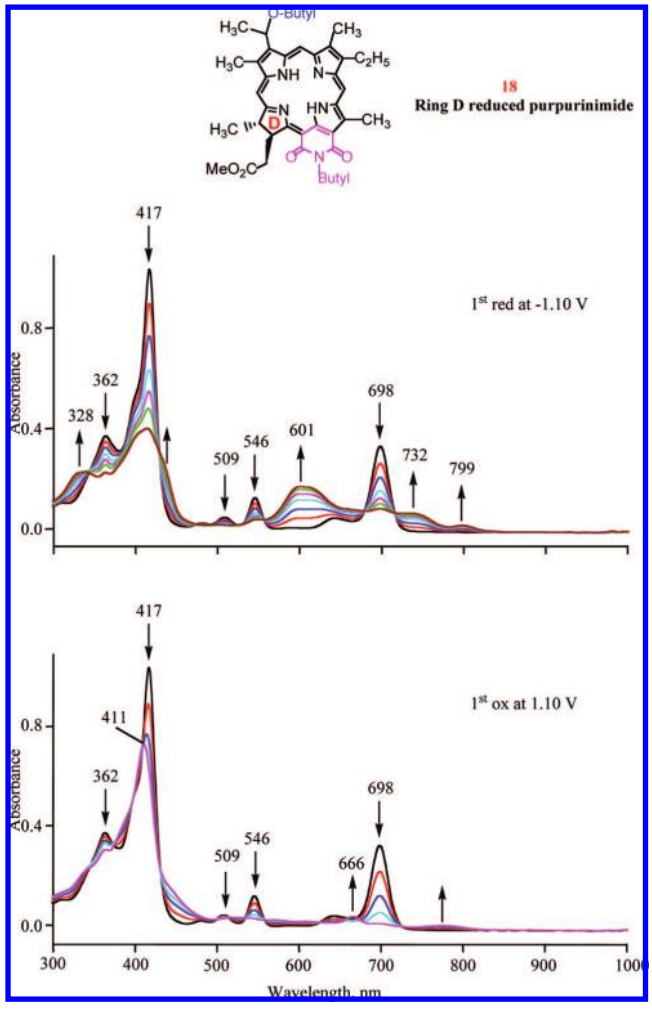


***Figure 11.*** Spectral changes of **18** during the first reduction and first oxidation in $CH_2Cl_2$ containing 0.2 M TABP.

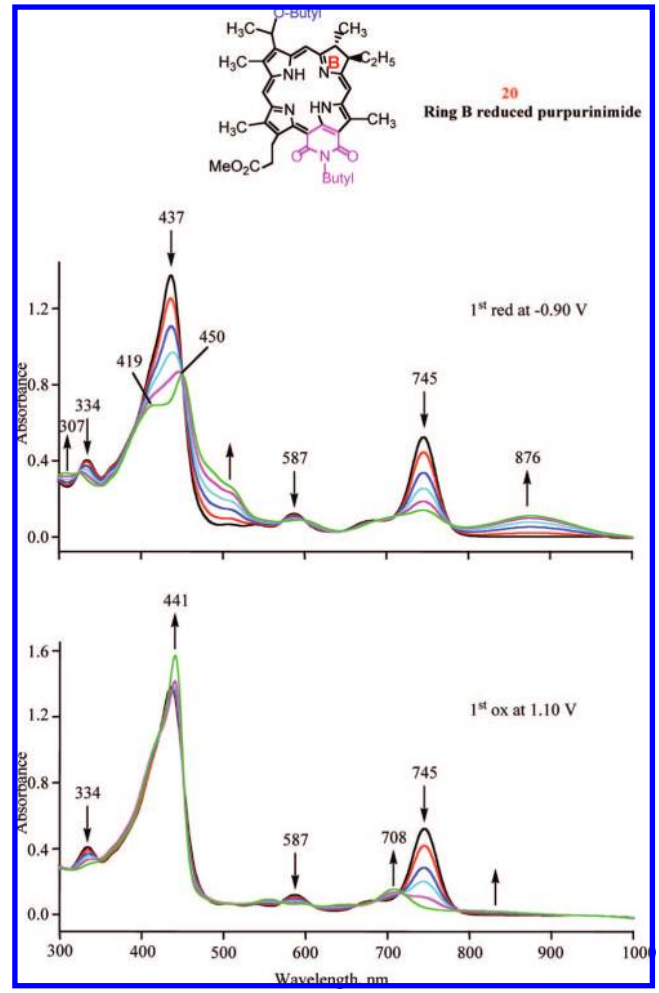


***Figure 12.*** Spectral changes of **20** during the first reduction and first oxidation in $CH_2Cl_2$ containing 0.2 M TABP.

ring and reduced B or D ring (**17** and **18**, **11** and **10**), the differences amounting to only 7−9 nm.

Figure 11 shows the UV−visible spectral changes for compound **18** upon the first reduction and first oxidation in $CH_2Cl_2$ containing 0.2 M TBAP. As can be seen in Figure 11, all bands of the neutral compound (362, 417, 509, 546, and 698 nm) decrease in intensity after a reducing potential of −1.10 V is applied, and four new bands characteristic of formation of a chlorin radical anion appear at 328, 601, 732, and 799 nm. This spectral behavior contrasts with what is seen for compound **20**, which has a reduced B ring and exhibits the spectral changes shown in Figure 12 during reduction. The bands of the initial compound at 334, 437, 587, and 745 nm decrease in intensity, and the peak at 437 nm splits into two bands at 419 and 450 nm. Simultaneously, a small band at 307 nm increases in intensity, and a broad new band appears at about 876 nm which is similar to a radical anion band often seen in singly reduced porphyrin macrocycles. This band is not seen for the other two compounds with a six-atom fused exocyclic ring, acetyl substituents (**14** and **13**), and reduced D and B rings (see Figures S5 and S6 in the Supporting Information). The intensity of all the UV−visible bands decreases during reduction of **13** and **14**. At the same time, three new bands at about 640, 780, and 850 nm increase in intensity during

the first reduction, and the product of the one-electron addition is assigned to a chlorin anion radical.

The four investigated compounds with a five-member fused ring, variable substituents, and different reduced D or B rings (**17**, **19**, **11**, and **10**) all exhibit similar UV−visible spectral changes upon the first reduction (Figures S7−S10, Supporting Information). The bands of the neutral compounds all decrease in intensity, and two or three new bands grow in at about 340, 620, and 800 nm. The ring-B reduced compounds exhibit broad red-shifted bands after the first reduction (for **19** at 798 nm and **10** at 850 nm) as compared to the chlorins with reduced D rings (for **17** at 779 nm and **11** at 817 nm). Compounds **11** and **10**, which have acetyl groups, display broad red-shifted bands compared to **17** and **19**, which have a hexyloxyethyl substituent.

The compounds with butyloxyethyl or hexyloxyethyl substituents and reduced D rings (**17** and **18**) show similar UV−visible spectral changes during the first oxidation in $CH_2Cl_2$, 0.2 M TBAP. After an oxidizing potential of 1.10 V is applied, all major bands of both compounds decrease in intensity, and a new broad band appears at about 800 nm, as shown in Figure 11 and Figure S7 (Supporting Information).

The other six chlorins (**19**, **14**, **13**, **20**, **11**, and **10**), which have different substituents and different exocyclic fused or reduced rings, all exhibit similar UV−visible spectral changes during the first oxidation. These spectral changes are shown in Figure 12 and in Figures S5, S6, S8, S9, and S10 in the Supporting Information. Upon application of a controlled oxidizing potential, the major band at about 420 nm increases in intensity as the other bands of the neutral compounds decrease in intensity. Compounds **20** and **19**, which have reduced B rings and butyloxyethyl or hexyloxyethyl substituent, show a broad band between 800 and 1000 nm, but this band is not seen for the other oxidized chlorins.

## Conclusions

This study reports the highly selective synthesis of ring-B reduced chlorins with a five-member isocyclic ring or a fused six-member *N*-butylimide ring. The latter compounds were synthesized using ferric chloride-mediated oxidation of the corresponding bacteriochlorins. Significant differences in the photophysical and electrochemical properties are seen between the ring-B reduced compounds and the ring-D reduced species with fused imide or isocyclic rings. Among the examined compounds, the ring-B reduced chlorin **20**, with a fused six-member *N*-butylimide ring, exhibits the most red-shifted absorption band at $\lambda_{max} = 746$ nm and the largest quantum yield for singlet oxygen formation (67%). An in vitro/in vivo biological evaluation of these new chlorins at variable light and drug doses is currently in progress. The smaller fluorescence quantum yields of the ring-B reduced form of chlorins as compared to those of the ring-D reduced forms found in this study may have something to do with the reason why nature selected the ring-D reduced chlorin (chlorophyll-*a*) and ring-B and -D reduced bacteriochlorins (bacteriochlorophyll-*a*) as chromophores in plant and bacterial photosynthetic reaction centers, respectively. In any case, the synthetic methods reported in this paper for preparation of the ring-B reduced chlorins should provide excellent opportunities to expand the scope of important chemical and biological functions of these type of compounds.

## Experimental Section

**General Procedures.** All reactions were carried out in flame-dried glassware under an atmosphere of nitrogen with magnetic stirring. Thin-layer chromatography (TLC) was done on ANALTECH precoated silica gel GF PE sheets (Cat. 159017, layer thickness 0.25 mm) and aluminum oxide NF PE sheets (Cat. 101016, layer thickness 0.2 mm). Column chromatography was performed over either silica gel 60 (70−230 mesh) or neutral alumina (Brockmann grade III, 50 mesh). In some cases, preparative TLC plates were also used for the purification (ANALTECH precoated silica gel GF glass plate, Cat. 02013, layer thickness 1.0 mm). Solvents were purified according to standard procedures. NMR spectra were recorded on a Bruker DRX 400 MHz spectrometer. All chemical shifts are reported in parts per million ($\delta$). $^1$H NMR (400 MHz) spectra were recorded at room temperature in $CDCl_3$ or $CD_3OD$ solutions and referenced to residual $CHCl_3$ (7.26 ppm) or TMS (0.00 ppm). ESI-mass spectra were carried out on a Brucker Esquire ion-trap mass spectrometer equipped with a pneumatically assisted electrospray ionization source, operating in positive mode. The high-resolution mass spectrometry analyses were performed at the Mass Spectrometry Facility, Michigan State University. UV−visible spectrums were recorded on Varian Cary 50 Bio UV−visible spectrophotometer using dichloromethane as solvent. All photophysical experiments were carried out using spectroscopic grade solvents.

**Methyl 3-Acetyl-3-de-ethyl-7,8-dihydrophylloerythrin (10).** Bacteriopyropheophorbide-*a* **5** (50.0 mg, 0.0883 mmol, 1.0 equiv) was dissolved in dichloromethane (50 mL). To this mixture was added slowly a nitromethane (4 mL) solution of $FeCl_3 \cdot 6H_2O$ (95.5 mg, 4.0 equiv). The resulting reaction mixture was stirred at room temperature for 10 min, quenched by addition of 20 mL of methanol, and washed with water three times. The organic layer was separated and dried over anhydrous $Na_2SO_4$, and solvent was removed under vacuum. The residue obtained was pure enough to proceed to the next step. Yield: 49.0 mg, 99%. $^1$H NMR (400 MHz, $CDCl_3$): $\delta$ 9.41 (s, 1H, 5-H), 9.32 (s, 1H, 10-H), 8.72 (s, 1H, 20-H), 5.44 (s, 2H, $13^1$-$CH_2$), 4.53 (q, $J = 4.8$ Hz, 1H, 7-H), 4.27 (br s, 1H, 8-H), 3.85 (t, $J = 6.8$ Hz, 2H, 17-$CH_2$), 3.75 (s, 3H, $COOCH_3$), 3.70 (s, 3H, 12-$CH_3$), 3.58 (s, 3H, 2-$CH_3$), 3.24 (s, 6H, 18-$CH_3$ + $CH_3CO$), 2.92 (t, $J = 7.2$ Hz, 2H, $17^1$-$CH_2$), 2.47−2.48 (m, 1H, $8^1$-H), 2.15−2.22 (m, 1H, $8^1$-H), 1.92 (d, $J = 6.8$ Hz, 3H, 7-$CH_3$), 0.89 (t, $J = 6.4$ Hz, 3H, $8^1$-$CH_3$), −0.68 (br s, 1H, NH), −1.61 (br s, 1H, NH). MS (ESI): *m*/*z* 565.3 (M + $H^+$). HRMS (ESI): calcd for $C_{34}H_{37}N_4O_4^+$ (M + $H^+$), 565.2815; found, 565.2824. UV−vis ($CH_2Cl_2$, $\lambda_{max}$, nm ($\epsilon$)): 691 ($4.31 \times 10^4$), 638 ($8.32 \times 10^3$), 550 ($9.78 \times 10^3$), 517 ($1.04 \times 10^4$), 415 ($7.39 \times 10^4$).

**Methyl 3-Acetyl-3-devinyl-pyropheophorbide-*a* (11).** Bacteriopyropheophorbide-*a* **5** (50.0 mg, 0.0883 mmol, 1.0 equiv) was dissolved in dichloromethane (50 mL). To this mixture was added slowly a $CH_2Cl_2$ (2 mL) solution of DDQ (87.0 mg, 4.0 equiv). The resulting reaction mixture was stirred at room temperature for 30 min and washed with water three times. The organic layer was separated and dried over anhydrous $Na_2SO_4$, and the solvent was removed under vacuum. The residue obtained was purified by flash column chromatography (silica gel, 3% acetone in $CH_2Cl_2$). This compound was previously reported by Tamiaki et al.[26] Yield: 46.0 mg, 92%. $^1$H NMR (400 MHz, $CDCl_3$): $\delta$ 9.98 (s, 1H, 5-H), 9.57 (s, 1H, 10-H), 8.77 (s, 1H, 20-H), 5.32 (d, $J = 20$ Hz, 1H, $13^2$-H), 5.17 (d, $J = 20$ Hz, 1H, $13^1$-$CH_2$), 4.56 (q, $J = 7.2$ Hz, 1H, 18-H), 4.36−4.38 (m, 1H, 17-H), 3.69−3.74 (m, 5H, 8-$CH_2$ + $COOCH_3$), 3.66 (s, 3H, 12-$CH_3$), 3.62 (s, 3H, 2-$CH_3$), 3.29 (s, 3H, 7-$CH_3$), 3.28 (s, 3H, $CH_3CO$), 2.70−2.77 (m, 1H, $17^1$-H), 2.56−2.64 (m, 1H, $17^1$-H), 2.29−2.35 (m, 2H, $17^1$-$CH_2$), 1.79 (d, $J = 7.2$ Hz, 3H, 18-$CH_3$), 1.71 (t, $J = 7.2$ Hz, 3H, $8^1$-$CH_3$), −2.02 (s, 1H, NH). MS (ESI): *m*/*z* 565.3 (M + $H^+$). UV−vis ($CH_2Cl_2$, $\lambda_{max}$, nm ($\epsilon$)):

683 (4.40 × $10^4$), 623 (6.37 × $10^3$), 547 (9.01 × $10^3$), 515 (9.97 × $10^3$), 418 (8.45 × $10^4$), 415 (6.46 × $10^4$).

**Methyl-3-acetyl-3-devinyl-*N*-butylimide-7,8-dihydroemeraldin (13).** The reaction of bacteriopurpurin-18-*N*-butylimide (**12**, 20.0 mg, 0.0307 mmol, 1.0 equiv) with $FeCl_3 \cdot 6H_2O$ (33.2 mg, 4.0 equiv) was carried out as discussed for compound **10**. Yield: 19.8 mg, 99%. $^1$H NMR (400 MHz, $CDCl_3$): $\delta$ 9.52 (s, 1H, 20-H), 9.42 (s, 1H, 5-H), 8.81 (s, 1H, 10-H), 4.40 (t, $J$ = 7.2 Hz, 3H, N-$CH_2$ + 7-H), 4.18−4.20 (m, 1H, 8-H), 3.79−3.94 (m 2H, 17-$CH_2$), 3.74 (s, 3H, $COOCH_3$), 3.66 (s, 3H, 12-$CH_3$), 3.61 (s, 3H, 2-$CH_3$), 3.18 (s, 3H, 18-$CH_3$), 3.16 (s, 3H, $CH_3CO$), 3.05 (t, $J$ = 10 Hz, 2H, $17^1$-$CH_2$), 2.39−2.47 (m, 1H, $8^1$-H), 2.05−2.12 (m, 1H, $8^1$-H), 1.93−2.00 (m, 2H, N-$CH_2CH_2$), 1.84 (d, $J$ = 7.6 Hz, 3H, 7-$CH_3$), 1.59−1.68 (m, 2H, N-$CH_2CH_2CH_2$), 1.08−1.13 (m, 6H, $8^1$-$CH_3$ + N-$(CH_2)_3CH_3$), −0.52 (br s, 2H, NH). MS (ESI): *m*/*z* 650.4 (M + $H^+$). HRMS (ESI): calcd for $C_{38}H_{44}N_5O_5^+$ (M + $H^+$), 650.3342; found, 650.3345. UV−vis ($CH_2Cl_2$, $\lambda_{max}$, nm ($\epsilon$)): 747 (3.64 × $10^4$), 681 (6.87 × $10^3$), 585 (8.97 × $10^3$), 544 (4.80 × $10^3$), 506 (6.71 × $10^3$), 440 (8.85 × $10^4$).

**Methyl-3-acetyl-3-devinyl-purpurin-18-*N*-butylimide (14).** Treatment of bacteriopurpurin-18-*N*-butylimide (**12**, 20.0 mg, 0.0307 mmol, 1.0 equiv) with DDQ (32.0 mg, 4.0 equiv) was done by the procedure described for the preparation of **11** and resulted in the desired product. Yield: 18.2 mg, 91%. $^1$H NMR (400 MHz, $CDCl_3$): $\delta$ 9.95 (s, 1H, 5-H), 9.66 (s, 1H, 10-H), 8.73 (s, 1H, 20-H), 5.42 (d, $J$ = 6.4 Hz, 1H, 17-H), 4.47 (t, $J$ = 7.6 Hz, 2H, N-$CH_2$), 4.39 (q, $J$ = 6.8 Hz, 1H, 18-H), 3.85 (s, 3H, $COOCH_3$), 3.66 (q, $J$ = 7.6 Hz, 2H, 8-$CH_2$), 3.60 (s, 3H, 12-$CH_3$), 3.57 (s, 3H, 2-$CH_3$), 3.24 (s, 3H, $CH_3CO$), 3.20 (s, 3H, 7-$CH_3$), 2.67−2.74 (m, 1H, $17^1$-H), 2.34−2.47 (m, 2H, $17^1$-$CH_2$), 1.93−2.04 (m, 3H, N-$CH_2CH_2$ + $17^1$-H), 1.78 (d, $J$ = 7.6 Hz, 3H, 18-$CH_3$), 1.62−1.70 (m, 5H, N-$CH_2CH_2CH_2$ + $8^1$-$CH_3$), 1.11 (t, $J$ = 7.6 Hz, 3H, N-$(CH_2)_3CH_3$), −0.23 (br s, 1H, NH), −0.35 (br s, 1H, NH). MS (ESI): *m*/*z* 650.3 (M + $H^+$). HRMS (ESI): calcd for $C_{38}H_{44}N_5O_5^+$ (M + $H^+$), 650.3342; found, 650.3338. UV−vis ($CH_2Cl_2$, $\lambda_{max}$, nm ($\epsilon$)): 726 (3.69 × $10^4$), 666 (5.62 × $10^3$), 555 (1.49 × $10^4$), 514 (4.49 × $10^3$), 419 (8.63 × $10^4$), 376 (4.27 × $10^4$).

**3-(1-Hydroxyethyl)-3-deacetyl-bacteriopurpurin-18-*N*-butylimide Methyl Ester (16).** Compound **12** (40.0 mg, 0.0108 mmol, 1.0 equiv) was dissolved in dichloromethane/methanol (20 mL, 4:1 v/v) and treated with sodium borohydride (10.8 mg, 4.0 equiv). The entire mixture was stirred at room temperature for 2 h. The reaction mixture extracted with dichloromethane and then was washed with water (3 × 200 mL). The organic layer was dried over anhydrous sodium sulfate. The residue obtained after evaporation was purified by flash column chromatography (silica gel, 5% acetone in $CH_2Cl_2$). Yield: 27.3 mg, 68%. $^1$H NMR (400 MHz, $CDCl_3$): $\delta$ 9.03 (s, 1H, 10-H), 9.01 (d, $J$ = 11.6 Hz, 5-H), 8.64 (s, 1H, 20-H), 6.38 (q, $J$ = 6.4 Hz, 1H, $3^1$-H), 5.20 (s, 2H, $13^1$-$CH_2$), 4.47−4.50 (m, 1H, 8-H), 4.22−4.24 (m, 1H, 7-H), 3.74 (s, 3H, $COOCH_3$), 3.51−3.57 (m, 5H, 17-$CH_2$ + 12-$CH_3$), 3.46 (d, 3H, 8-$CH_3$), 3.03 (d, 3H, 18-$CH_3$), 2.77−2.81 (m, 2H, $17^1$-$CH_2$), 2.45−2.52 (m, 1H, $8^1$-H), 2.16 (d, $J$ = 6.4 Hz, 4H, $8^1$-H + $3^1$-$CH_3$), 1.91−1.94 (m, 3H, 7-$CH_3$), 1.17−1.20 (m, 3H, $8^1$-$CH_3$), −0.55 (br s, 1H, NH), −1.66 (br s, 1H, NH). MS (ESI): *m*/*z* 567.5 (M + $H^+$). HRMS (ESI): calcd for $C_{34}H_{39}N_4O_4^+$ (M + $H^+$), 567.2971; found, 565.2968. UV−vis ($CH_2Cl_2$, $\lambda_{max}$, nm ($\epsilon$)): 669 (3.41 × $10^4$), 611 (5.57 × $10^3$), 539 (5.39 × $10^3$), 512 (9.01 × $10^3$), 410 (7.03 × $10^4$).

**Methyl 3-(1-Hexyloxyethyl)-3-de-ethyl-7,8-dihydrophylloerythrin (19).** Following the procedure described for the preparation of **10**, compound **23** (40.0 mg, 0.0705 mmol, 1.0 equiv) was treated with $FeCl_3 \cdot 6H_2O$ (66.3 mg, 4.0 equiv), resulting in the desired product. Purification of the reaction mixture was done by flash column chromatography (silica gel, 30% ethyl acetate in petrol ether). Yield: 33.0 mg, 71%. $^1$H NMR (400 MHz, $CDCl_3$): $\delta$ 9.18 (s, 1H, 10-H), 9.04/9.01 (s, 1H, 5-H), 8.65 (s, 1H, 20-H), 5.79−5.86 (m, 1H, $3^1$-H), 5.48 (s, 2H, $13^1$-$CH_2$), 4.41−4.50 (m, 1H, 8-H), 4.20−4.22 (m, 1H, 7-H), 3.90 (t, $J$ = 8.0 Hz, 2H, 17-$CH_2$), 3.75 (s, 3H, $COOCH_3$), 3.52−3.66 (m, 5H, $3^1$-$OCH_2$ + 12-$CH_3$), 3.44/3.43 (s, 3H, 2-$CH_3$), 3.23 (s, 3H, 18-$CH_3$), 2.94 (t, $J$ = 8.0 Hz, 2H, $17^1$-$CH_2$), 2.42−2.52 (m, 1H, $8^1$-H), 2.13−2.20 (m, 1H, $8^1$-H), 2.10 (d, $J$ = 6.8 Hz, 3H, $3^1$-$CH_3$), 1.91/1.87 (d, $J$ = 7.2 Hz, 3H, 7-$CH_3$), 1.66−1.76 (m, 3H, $3^1$-$OCH_2CH_2$), 1.15−1.23 (m, 9H, $3^1$-$OCH_2CH_2CH_2CH_2CH_2CH_3$), 0.78−0.81 (m, 3H, $8^1$-$CH_3$), −0.34 (br s, 1H, NH), −1.52 (br s, 1H, NH). MS (ESI) *m*/*z*: 651.4 (M + $H^+$). HRMS (ESI): calcd for $C_{40}H_{51}N_4O_4^+$ (M + $H^+$), 651.3910; found, 651.3906. UV−vis ($CH_2Cl_2$, $\lambda_{max}$, nm ($\epsilon$)): 669 (4.45 × $10^4$), 612 (6.77 × $10^3$), 540 (6.77 × $10^3$), 513 (1.11 × $10^4$), 411 (7.82 × $10^4$).

**3-(1-Butyloxyethyl)-3-de-ethyl-7,8-dihydro-*N*-butyl-emeraldine (20).** Using the procedure described for the preparation of **10**, the purpurinimide **24** (40.0 mg, 0.0705 mmol, 1.0 equiv) was treated with $FeCl_3 \cdot 6H_2O$ (66.3 mg, 4.0 equiv), affording the desired product. Purification was done by flash column chromatography (silica gel, 30% ethyl acetate in petrol ether). Yield: 33.0 mg, 71%. $^1$H NMR (400 MHz, $CDCl_3$): $\delta$ 9.18 (s, 1H, 5-H), 9.04/9.01 (s, 1H, 10-H), 8.65 (s, 1H, 20-H), 5.79−5.86 (m, 1H, $3^1$-H), 5.48 (s, 2H, $13^1$-$CH_2$), 4.41−4.50 (m, 1H, 8-H), 4.20−4.22 (m, 1H, 7-H), 3.90 (t, $J$ = 8.0 Hz, 2H, 17-$CH_2$), 3.75 (s, 3H, $COOCH_3$), 3.52−3.66 (m, 5H, $3^1$-$OCH_2$ + 12-$CH_3$), 3.44/3.43 (s, 3H, 2-$CH_3$), 3.23 (s, 3H, 18-$CH_3$), 2.94 (t, $J$ = 8.0 Hz, 2H, $17^1$-$CH_2$), 2.42−2.52 (m, 1H, $8^1$-H), 2.13−2.20 (m, 1H, $8^1$-H), 2.10 (d, $J$ = 6.8 Hz, 3H, $3^1$-$CH_3$), 1.91/1.87 (d, $J$ = 7.2 Hz, 3H, 7-$CH_3$), 1.66−1.76 (m, 3H, $3^1$-$OCH_2CH_2$), 1.15−1.23 (m, 9H, $3^1$-$OCH_2CH_2CH_2CH_2CH_2CH_3$), 0.78−0.81 (m, 3H, $8^1$-$CH_3$), −0.34 (br s, 1H, NH), −1.52 (br s, 1H, NH). MS (ESI): *m*/*z* 651.4 (M + $H^+$). HRMS (ESI): calcd for $C_{40}H_{51}N_4O_4^+$ (M + $H^+$), 651.3910; found, 651.3906. UV−vis ($CH_2Cl_2$, $\lambda_{max}$, nm ($\epsilon$)): 669 (4.45 × $10^4$), 612 (6.77 × $10^3$), 540 (6.77 × $10^3$), 513 (1.11 × $10^4$), 411 (7.82 × $10^4$).

**Methyl 3-(1-Hexyloxyethyl)-3-de-ethyl-7,8-dihydrophylloerythrin (21).** Compound **19** (20 mg, 0.0307 mmol, 1.0 equiv) was dissolved in degassed THF (10 mL). Degassed water and a solution of $LiOH \cdot H_2O$ (51.6 mg, 40 equiv) in methanol (10 mL, 1:1 v/v) were added. The entire reaction mixture was then stirred under nitrogen atmosphere at room temperature for 2 h, and the resulting mixture was diluted with dichloromethane (20 mL). The reaction mixture was washed three times with water. The organic layer was separated and dried over $Na_2SO_4$, and the solvent was removed under reduced pressure. The residue obtained was purified by flash column chromatography (silica gel, 5% methanol in $CH_2Cl_2$). Yield: 16.6 mg, 85%. $^1$H NMR (400 MHz, $CDCl_3$): $\delta$ 9.16 (s, 1H, 5-H), 9.06/9.02 (s, 1H, 10-H), 8.64/8.62 (s, 1H, 20-H), 5.81−5.87 (m, 1H, $3^1$-H), 5.37/5.36 (s, 2H, $13^1$-$CH_2$), 4.41−4.50 (m, 1H, 7-H), 4.19−4.23 (m, 1H, 8-H), 3.79 (t, $J$ = 8.4 Hz, 2H, 17-$CH_2$), 3.57−3.69 (m, 2H, $3^1$-$OCH_2$), 3.55 (s, 3H, 12-$CH_3$), 3.45 (s, 3H, 2-$CH_3$), 3.20 (s, 3H, 18-$CH_3$), 2.96 (t, $J$ = 8.4 Hz, 2H, $17^1$-$CH_2$), 2.43−2.51 (m, 1H, $8^1$-H), 2.12 (d, $J$ = 6.8 Hz, 4H, $3^1$-$CH_3$ + $8^1$-H), 1.93/1.89 (d, $J$ = 7.6 Hz, 3H, 7-$CH_3$), 1.68−1.78 (m, 2H, $3^1$-$OCH_2CH_2$), 1.16−1.25 (m, 9H, $3^1$-$OCH_2CH_2CH_2$ $CH_2$ $CH_2CH_3$), 0.80 (t, $J$ = 7.2 Hz, 3H, $8^1$-$CH_3$), −0.34 (br s, 1H, NH), −1.52 (br s, 1H, NH). MS (ESI): *m*/*z* 637.5 (M + $H^+$). HRMS (ESI): calcd for $C_{39}H_{49}N_4O_4^+$ (M + $H^+$), 637.3754; found, 637.3749. UV−vis ($CH_2Cl_2$, $\lambda_{max}$, nm ($\epsilon$)): 668 (6.1 × $10^4$), 612 (1.0 × $10^4$), 540 (1.0 × $10^4$), 514 (1.7 × $10^4$), 413 (12.0 × $10^4$).

**Methyl 3-(1-Hydroxyethyl)-3-deacetyl-bacteriopyropheophorbide-*a* (22).** Bacteriopyropheophorbide-*a* **5** (50.0 mg, 0.0883 mmol, 1.0 equiv) was dissolved in dichloromethane/methanol (25 mL, 4:1 v/v). Sodium borohydride (33.6 mg, 10 equiv) was added. The entire mixture was stirred at room temperature for 2 h and washed thoroughly with saturated $NaHCO_3$ solution, brine, and water successively. The organic layer was separated and dried over $Na_2SO_4$. The organic layer was evaporated to dryness, and the resulting crude was pure enough to proceed for the next step. Yield: 49.0 mg, 98%. $^1$H NMR (400 MHz, $CDCl_3$): $\delta$ 8.51 (s, 1H, 5-H), 8.22 (s, 1H, 10-H), 8.02 (s, 1H, 20-H), 6.18 (q, $J$ = 5.6 Hz, 1H, $3^1$-H), 4.96 (d, $J$ = 20 Hz, 1H, $13^2$-H), 4.78 (d, $J$ = 20 Hz, 1H, $13^1$-H), 4.12−4.16 (m, 2H, 7-H + 18-H), 3.98−4.00 (m, 1H, 17-

H), 3.88−3.90 (m, 1H, 8-H), 3.62 (s, 3H, $COOCH_3$), 3.35 (s, 3H, 12-$CH_3$), 3.21 (s, 3H, 2-$CH_3$), 2.17−2.57 (m, 6H, $8^1$-$CH_2$ + 17-$CH_2$ + $17^1$-$CH_2$), 2.04 (d, $J$ = 6.4 Hz, 3H, $3^1$-$CH_3$), 1.66−1.77 (m, 6H, 7-$CH_3$ + 18-$CH_3$), 1.12 (t, $J$ = 7.2 Hz, 3H, $8^1$-$CH_3$), −0.22 (s, 1H, NH). MS (ESI): $m/z$ 569.4 ($M + H^+$). UV−vis ($CH_2Cl_2$, $\lambda_{max}$, nm): 717, 654, 602, 516, 499, 486, 351.

**Methyl 3-(1-Hexyloxyethyl)-3-deacetyl-bacteriopyrropheophorbide-*a* (23).** Compound **22** (50.0 mg, 0.0879 mmol, 1.0 equiv) was dissolved in dry $CH_2Cl_2$ (6 mL), and HBr gas was bubbled into the solution for 2 min. The reaction mixture was stirred for 5 min at room temperature. The solvent was evaporated under high vacuum, the resulting crude was dried, and the entire crude was dissolved in dry $CH_2Cl_2$ (4 mL). A 25 mg portion of dry $K_2CO_3$ was added to this mixture, followed by addition of $C_6H_{13}OH$ (0.1 mL). The resulting reaction mixture was stirred for 30 min at room temperature and then worked up. Purification of the crude mixture was done by flash column chromatography (silica gel, 50% ethyl acetate in hexane). Yield: 43.0 mg, 75%. $^1$H NMR (400 MHz, $CDCl_3$): $\delta$ 8.55/8.52/8.51 (s, 1H, 5-H), 8.20 (s, 1H, 10-H), 7.99 (s, 1H, 20-H), 5.60−5.66 (m, 1H, $3^1$-H), 4.96 (d, $J$ = 20.0 Hz, 1H, $13^1$-H), 4.78 (d, $J$ = 20.0 Hz, 1H, $13^1$-H), 4.09−4.15 (m, 2H, 7-H + 8-H), 3.99 (d, 1H, 17-H), 3.87−3.89 (m, 1H, 8-H), 3.62 (s, 3H, $COOCH_3$), 3.51−3.59 (m, 2H, $3^1$-$OCH_2$), 3.35 (s, 3H, 12-$CH_3$), 3.15 (s, 3H, 2-$CH_3$), 2.44−2.57 (m, 2H, $8^1$-H + $17^1$-H), 2.19−2.33 (m, 3H, $17^1$-H + $17^1$-$CH_2$), 1.99−2.02 (m, 1H, $8^1$-H), 1.98 (d, $J$ = 6.4 Hz, 3H, $3^1$-$CH_3$), 1.67−1.78 (m, 8H, 7-$CH_3$ + 18-$CH_3$ + $3^1$-$OCH_2CH_2$), 1.24−1.36 (m, 6H, $3^1$-$OCH_2CH_2(CH_2)_3$), 1.10−1.15 (m, 3H, $3^1$-$O(CH_2)_5CH_3$), 0.82 (t, $J$ = 6.0 Hz, 3H, $8^1$-$CH_3$). MS (ESI): $m/z$ 653.5 ($M + H^+$). HRMS (ESI): calcd for $C_{40}H_{53}N_4O_4^+$ ($M + H^+$), 653.4067; found, 653.4058. UV−vis ($CH_2Cl_2$, $\lambda_{max}$, nm ($\epsilon$)): 717 ($3.46 \times 10^4$), 655 ($1.25 \times 10^4$), 603 ($5.12 \times 10^3$), 516 ($2.68 \times 10^4$), 485 ($7.17 \times 10^3$), 456 ($2.94 \times 10^3$), 382 ($4.73 \times 10^4$), 355 ($9.06 \times 10^4$).

**3-(1′-Butyloxyethyl)-3-deacetyl-bacteriopurpurin-18-*N*-butylimide Methyl Ester (24).** Following the procedure described for the preparation of **19**, mixing bacteriochlorin **16** (40.0 mg, 0.0613 mmol, 1.0 equiv) with $C_4H_9OH$ (0.1 mL) and $K_2CO_3$ (20.0 mg) resulted in the desired product. Purification was done by flash column chromatography (silica gel, 25% ethyl acetate in petroleum ether). Yield: 28.2 mg, 65%. $^1$H NMR (400 MHz, $CDCl_3$): $\delta$ 9.60 (s, 1H, 10-H), 9.33/9.28 (s, 1H, 5-H), 9.02 (s, 1H, 20-H), 5.81−5.89 (m, 1H, $3^1$-H), 4.47 (t, $J$ = 7.2 Hz, 3H, N-$CH_2$ + 7-H), 4.33 (br s, 1H, 8-H), 3.94−4.05 (m 2H, 17-$CH_2$), 3.84 (s, 3H, $COOCH_3$), 3.62 (s, 4H, 12-$CH_3$ + O-$CH_2$), 3.52/3.51 (s, 4H, 2-$CH_3$ + O-$CH_2$), 3.25 (s, 3H, 18-$CH_3$), 3.13 (t, $J$ = 8.8 Hz, 2H, $17^1$-$CH_2$), 2.43−2.52 (m, 1H, $8^1$-H), 2.11−2.18 (m, 4H, $3^1$-H + $8^1$-H), 1.99−2.06 (m, 2H, N-$CH_2CH_2$), 1.90 (t, $J$ = 7.6 Hz, 3H, 7-$CH_3$), 1.63−1.75 (m, 4H, N-$CH_2CH_2CH_2$ + O-$CH_2CH_2$), 1.33−1.44 (m, 2H, O-$CH_2$-$CH_2CH_2$), 1.10−1.16 (m, 6H, $O(CH_2)_3CH_3$ + $N(CH_2)_3CH_3$), 0.82−0.87 (m, 3H, $8^1$-$CH_3$), −1.64 (br s, 2H, NH). MS (ESI): $m/z$ 708.6 ($M + H^+$). HRMS (ESI): calcd for $C_{42}H_{54}N_5O_5^+$ ($M + H^+$), 708.4125; found, 708.4128. UV−vis ($CH_2Cl_2$, $\lambda_{max}$, nm ($\epsilon$)): 746 ($3.15 \times 10^4$), 682 ($4.91 \times 10^3$), 587 ($7.08 \times 10^3$), 539 ($3.78 \times 10^3$), 539 ($3.78 \times 10^3$), 508 ($3.86 \times 10^3$), 436 ($7.93 \times 10^4$).

**Electrochemical and Spectroelectrochemical Measurements.** Cyclic voltammetry (CV) measurements were performed at 298 K on an EG&G model 173 potentiostat coupled with an EG&G model 175 universal programmer in deaerated dichloromethane ($CH_2Cl_2$) solution containing 0.1 M tetra-*n*-butylammonium perchlorate (TBAP) as a supporting electrolyte. A three-electrode system was utilized and consisted of a glassy carbon working electrode, a platinum wire counter electrode, and a saturated calomel reference electrode (SCE). The reference electrode was separated from the bulk of the solution by a fritted-glass bridge filled with the solvent/supporting electrolyte mixture. Thin-layer spectroelectrochemical measurements were carried out using an optically transparent platinum thin-layer working electrode and a Hewlett-Pachard model 8453 diode array spectrophotometer coupled with an EG&G model 173 universal programmer.

**Photophysical Measurements.** Absorption spectra were recorded on a Hewlett-Packard 8453A diode array spectrophotometer. Time-resolved fluorescence spectra were measured by a Photon Technology International GL-3300 with a Photon Technology International GL-302 nitrogen laser/pumped dye laser system, equipped with a four-channel digital delay/pulse generator (Stanford Research System Inc. DG535) and a motor driver (Photon Technology International MD-5020). Excitation wavelengths were from 538 to 551 nm using coumarin 540A (Photon Technology International, Canada) as a dye. Fluorescence lifetimes were determined by a single-exponential curve fit using a microcomputer. Fluorescence quantum yields of dye thin films were determined by the photoluminescence (PL) method using a Hamamatsu DynaSpect C 9920-02 absolute PL quantum yield measurement system, which is made up of an excitation light source (150 W xenon lamp), a monochromator, an integrating sphere, and a multichannel spectrometer. Singlet oxygen phosphorescence measurements were performed for an $O_2$-saturated $C_6D_6$ solution containing the sample in a quartz cell (optical path length 10 mm), which was excited at 532 nm using a Cosmo System LVU-200S spectrometer. A photomultiplier (Hamamatsu Photonics, R5509-72) was used to detect emission in the near-infrared region (band path 1 mm). All experiments were performed at 298 K.

**Calculations.** Theoretical calculations of the properties of molecules were performed using density functional theory (DFT) with the B3LYP density functional[32] and the 3-21G* basis set. All calculations were performed using GAUSSIAN-03.[33] Graphical outputs of the computational results were generated with the Gauss View software program (ver. 3.09) developed by Semichem, Inc.[34]

**Acknowledgment.** This work was supported by a Grant-in-Aid (Nos. 19205019 and 19750034) a Global COE program, "the Global Education and Research Center for Bio-Environmental Chemistry", from the Ministry of Education, Culture, Sports, Science and Technology, Japan; the Robert A. Welch Foundation (K.M.K., Grant E-680); NIH (CA 55791, 1RO1CA127369-01A1, R21 CA109914, R21/33 CA114053, and Roswell Park Alliance Foundation), and the shared resources of the Roswell Park Cancer Center Support Grant (P30CA16056). Mass spectrometry analyses were performed at the Mass Spectrometry Facility, Michigan State University, East Lansing, MI.

**Supporting Information Available:** $^1$H NMR data in $CDCl_3$, DFT calculation, and spectroelectrochemical results, and complete ref 33. This material is available free of charge via the Internet at http://pubs.acs.org.

JA8050298

(34) Dennington, R., II; Keith, T.; Millam, J.; Eppinnett, K.; Hovell, W. L.; Gilliland, R. *Gaussview*; Semichem, Inc.: Shawnee Mission, KS, 2003.